

Temperate and chronic virus competition leads to low lysogen frequency

Sara M. Clifton*

*Department of Mathematics, Statistics, and Computer Science,
St. Olaf College, Northfield, Minnesota 55057, USA*

Rachel J. Whitaker

*Department of Microbiology, University of Illinois at
Urbana-Champaign, Urbana, Illinois 61801, USA and
Carl R. Woese Institute for Genomic Biology,
University of Illinois at Urbana-Champaign, Urbana, Illinois 61801, USA*

Zoi Rapti

*Department of Mathematics, University of Illinois at
Urbana-Champaign, Urbana, Illinois 61801, USA and
Carl R. Woese Institute for Genomic Biology,
University of Illinois at Urbana-Champaign, Urbana, Illinois 61801, USA*

Abstract

The canonical bacteriophage is obligately lytic: the virus infects a bacterium and hijacks cell functions to produce large numbers of new viruses which burst from the cell. These viruses are well-studied, but there exist a wide range of coexisting virus lifestyles that are less understood. Temperate viruses exhibit both a lytic cycle and a latent (lysogenic) cycle, in which viral genomes are integrated into the bacterial host. Meanwhile, chronic (persistent) viruses use cell functions to produce more viruses without killing the cell; chronic viruses may also exhibit a latent stage in addition to the productive stage. Here, we study the ecology of these competing viral strategies. We demonstrate the conditions under which each strategy is dominant, which aids in control of human bacterial infections using viruses. We find that low lysogen frequencies provide competitive advantages for both virus types; however, chronic viruses maximize steady state density by eliminating lysogeny entirely, while temperate viruses exhibit a non-zero ‘sweet spot’ lysogen frequency. Viral steady state density maximization leads to coexistence of temperate and chronic viruses, explaining the presence of multiple viral strategies in natural environments.

* clifto2@stolaf.edu

I. INTRODUCTION

All viruses depend upon their hosts for reproduction. Viruses have evolved many strategies to reproduce within bacteria, including the lytic, temperate, and chronic lifestyles within the bacterial host [1–3]. After infection, lytic viruses replicate within the bacterial host and transmit by bursting from the cell, killing the host. Temperate viruses have both a lytic cycle and a latent cycle, in which the viral genetic material is integrated into host genomes; latent viruses remain dormant in the bacterial genome until induced to replicate [3]. In chronic infection, productive host cells bud new viruses from the cell without killing the bacterium [4]. Chronic viruses may also have a latent cycle in which viral genetic material is incorporated into the bacterium’s genome, and the cell transmits the virus’s genetic material (provirus) to daughter cells vertically [5]. Comparative genomics among closely related bacterial strains has uncovered a plethora of proviruses of both temperate and chronic lifestyles [6–11].

Viruses of all four lifestyle classes infect many bacteria relevant to human disease treatment, especially immunocompromised patients vulnerable to common bacterial infections. In particular, patients with cystic fibrosis or serious burns may become infected with the ubiquitous *Pseudomonas aeruginosa*, which can lead to patient death within days if unsuccessfully treated [12–14]. Because *P. aeruginosa* is often resistant to multiple antibiotic treatments [15–17], phage therapy [18, 19] and phage-antibiotic synergistic (PAS) therapy [20–22] are now being studied to treat bacterial infections. Response to these treatments depends significantly on the ecology of the bacteria-virus system already present within the human host [23]; therefore it is critical to understand the environmental and evolutionary conditions under which each viral strategy is dominant in order to provide effective treatment.

While mathematical models of lytic viruses (e.g., [24, 25]) and temperate viruses (e.g., [26]) have been studied extensively, relatively few models of chronic viruses (e.g., [23, 27, 28]) have been examined. To our knowledge, no studies have rigorously analyzed the ecological interactions among bacteria and all four viral lifestyles: lytic, latent lytic, chronic, and latent chronic. Several important open questions exist that neither experimental nor modeling efforts have yet answered in this context:

1. Experiments have found that temperate virus lysogen frequencies tend to be small ($\sim 1\%$ of infections) [1]. What are the theoretical underpinnings of this phenomenon?
2. Lysogen frequencies for temperate viruses have been well-studied both experimentally and theoretically [1, 29, 30], but lysogen frequencies for chronic viruses have not been determined. What is the predicted range of lysogen frequencies for chronic viruses?
3. Bacterial recovery (cure) rates from viral infection have not been quantified either experimentally or theoretically. Most mathematical models ignore recovery for simplicity (e.g., [28]). Experimentally, a wide range of recovery rates has been observed; some proviruses remain viable over evolutionary timescales (implying recovery rates near zero) [31], and some proviruses are inactivated nearly instantly by CRISPR systems (implying extremely fast recovery rates) [32]. Can we establish a narrower range of typical recovery rates?

In this paper we develop a mathematical model of the competition between temperate and chronic viruses for bacterial hosts, using *P. aeruginosa* infections within humans as

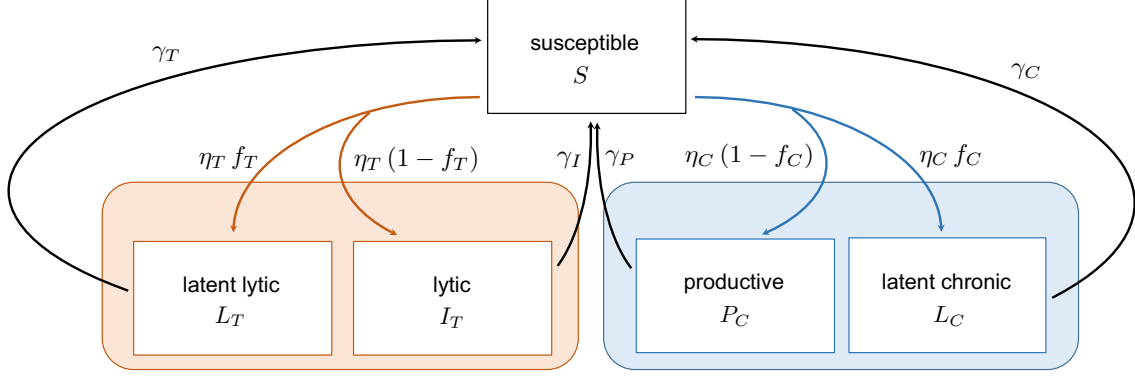


FIG. 1. Flowchart of model equations (1-7). Arrows indicate infection by temperate viruses (orange), infection by chronic viruses (blue), or recovery from infection (black). Infection rates are denoted η_i , recovery (cure) rates are denoted γ_i , and lysogen frequencies are denoted f_i .

motivation. An analysis of this model yields simple and intuitive answers to the preceding questions.

II. MODEL

With the goal of understanding competition between two viral strategies, temperate viruses V_T with lytic and latent lytic stages and chronic viruses V_C with productive and latent chronic stages, we develop a simple model of the bacteria-virus ecosystem (see Figure 1 for the model overview). Each virus may infect a single strain of bacteria that is initially susceptible (S) to both viral types. We assume the total bacterial population N grows logistically to a carrying capacity K [33]. Susceptible bacteria grow at a rate r_S , and infected bacteria may grow at either faster or slower rates [34].

Temperate viruses infect susceptible bacteria at a rate η_T ; the infected bacteria will either become latently infected L_T with probability f_T , or will enter a lytic state I_T with probability $1 - f_T$. Bacteria in the lytic state produce viruses and burst (with burst size β_T) at a rate δ . While in the lytic state, the virus hijacks cell functions, and the cell cannot reproduce [35, 36]. Bacteria in the latent lytic state reproduce at a rate r_T . Bacteria do not move between lytic and latent states unless the system is stressed (e.g., by heat or sublethal antibiotics); we ignore spontaneous induction because it is a rare occurrence [37–39]. However, lytic and latent lytic bacteria may recover from infection at rate γ_I and γ_T , respectively [31, 40].

Similarly, chronic viruses infect susceptible bacteria at a rate η_C , leading to either latent infection L_C with probability f_C or productive infection P_C with probability $1 - f_C$ [41]. Bacteria in the productive state reproduce at a rate r_P and produce viruses at a rate β_C without cell death. While in the latent chronic state, bacteria reproduce at a rate r_C . Unless the system is stressed, bacteria will not switch from latent to productive states, but productive and latent chronic bacteria may recover at rate γ_P and γ_C , respectively [31, 40]. Again, we ignore spontaneous induction due to its rarity [37–39].

Once a bacterium is infected, we assume it will exclude both superinfection by the same viral type and cross infection by viruses of the other type [42]. Outside the cell, free temperate viruses and free chronic viruses decay naturally at rates μ_T and μ_C , respectively

[43].

The following equations (1-7) are the dynamical systems model that captures the preceding qualitative description. See Table I for variable descriptions and Table II for parameter descriptions and relevant values.

$$\dot{S} = \underbrace{r_S S \left(1 - \frac{N}{K}\right)}_{\text{growth}} - \underbrace{\eta_T S V_T - \eta_C S V_C}_{\text{infection}} + \underbrace{\gamma_T L_T + \gamma_I I_T + \gamma_P P_C + \gamma_C L_C}_{\text{recovery}} \quad (1)$$

$$\dot{I}_T = \underbrace{\eta_T (1 - f_T) S V_T}_{\text{infection}} - \underbrace{\delta I_T}_{\text{lysis}} - \underbrace{\gamma_I I_T}_{\text{recovery}} \quad (2)$$

$$\dot{L}_T = \underbrace{r_T L_T \left(1 - \frac{N}{K}\right)}_{\text{growth}} + \underbrace{\eta_T f_T S V_T}_{\text{infection}} - \underbrace{\gamma_T L_T}_{\text{recovery}} \quad (3)$$

$$\dot{P}_C = \underbrace{r_P P_C \left(1 - \frac{N}{K}\right)}_{\text{growth}} + \underbrace{(1 - f_C) \eta_C S V_C}_{\text{infection}} - \underbrace{\gamma_P P_C}_{\text{recovery}} \quad (4)$$

$$\dot{L}_C = \underbrace{r_C L_C \left(1 - \frac{N}{K}\right)}_{\text{growth}} + \underbrace{f_C \eta_C S V_C}_{\text{infection}} - \underbrace{\gamma_C L_C}_{\text{recovery}} \quad (5)$$

$$\dot{V}_T = \underbrace{\beta_T \delta I_T}_{\text{burst}} - \underbrace{\eta_T S V_T}_{\text{adsorption}} - \underbrace{\mu_T V_T}_{\text{degradation}} \quad (6)$$

$$\dot{V}_C = \underbrace{\beta_C P_C}_{\text{production}} - \underbrace{\eta_C S V_C}_{\text{adsorption}} - \underbrace{\mu_C V_C}_{\text{degradation}} \quad (7)$$

TABLE I. Description of model variables in bacteria-virus system (1-7). Due to nondimensionalization of density and time, all variables and parameters are nondimensional; all densities are relative to the bacterial carrying capacity and all rates are relative to the growth rate of uninfected bacteria.

Variable	Meaning
S	density of susceptible bacteria
I_T	density of lytic bacteria preparing to burst
L_T	density of latent lytic bacteria
P_C	density of productive bacteria
L_C	density of latent chronic bacteria
N	density of all bacteria ($S + I_T + L_T + P_C + L_C$)
V_T	density of free temperate viruses
V_C	density of free chronic viruses
t	time normalized by bacterial reproduction rate

Note that infection rates for temperate and chronic viruses, although assumed constant, may depend on the bacterial population; many relevant bacteria form biofilms at high density that protect the population from infection [53]. For simplicity, we have also assumed

TABLE II. Description of model parameters in bacteria-virus system (1-7). Due to nondimensionalization of density and time, all variables and parameters are nondimensional; all densities are relative to the bacterial carrying capacity and all rates are relative to the growth rate of uninfected bacteria.

Parameter	Meaning	Range ^a	Baseline	Sources
r_S	net growth rate of susceptible bacteria, normalized to 1	1 ^b	1	[44]
r_T, r_P, r_C	growth rates of (respectively) latent lytic, productive, and latent chronic bacteria	[0.5, 3] ^c	1	[34, 45]
K	carrying capacity of bacteria, normalized to 1	1	1	
η_T, η_C	infection rate of (respectively) temperate and chronic viruses	[0.38, 14.7] ^d	1	[26]
$\gamma_T, \gamma_P, \gamma_C$	recovery rates of (respectively) latent lytic, productive, and latent chronic bacteria	[0, 1000] ^e	0.67 ^f	[31, 32]
γ_I	recovery rates of lytic bacteria	[0, 1000]	0 ^g	[31, 32]
δ	rate at which lytic infection leads to bursting (eclipse and rise phase)	[1.5, 7.8] ^h	4	[46, 47]
f_T	lysogen frequency for temperate viruses	[0, 0.9]	0.01	[1, 29, 30]
f_C	lysogen frequency for chronic viruses	[0, 0.9]	0 ^f	[1, 29, 30]
β_T	burst size for bacteria infected with V_T	[10, 1000]	100	[46–52]
β_C	viral production rate for bacteria infected with V_C	[5, 200]	20	[23]
μ_T, μ_C	degradation rate of (respectively) free temperate viruses and free chronic viruses	[0.9, 3.6] ⁱ	1	[43]

^aall parameter ranges are taken for the human pathogens *P. aeruginosa* or *E. coli* and their viruses, unless otherwise noted.

^bgrowth rate is approximately $5.1\text{e-}3 \text{ min}^{-1}$ for *P. aeruginosa* grown *in vitro*.

^cestimates based on *E. coli* and M13 phage.

^destimates based on *E. coli* and λ phage.

^ea wide range of recovery rates has been found; some proviruses are viable over evolutionary timescales and some proviruses are inactivated nearly instantly by CRISPR systems.

^festimated from viral steady state density (see Results section).

^gselected to be 0 to simplify model analysis; allowing $\gamma_I = \gamma_T$ produces qualitatively similar results, so the increased model complexity is not justified.

^hlow estimate is for PAXYB1 phage and PAO1 host, high estimate is for PAK_P3 phage and PAO1 host.

ⁱlow estimate is for viruses extracted from Raunefjorden, high estimate is for viruses extracted from Bergen Harbor (strains unknown).

that lysogen frequencies are constant, but some studies have demonstrated that bacterial density may impact lysogeny rates [54, 55]. These simplifications are necessary for analytic

tractability.

III. RESULTS

Although this model is applicable to any bacteria-virus ecosystem with both temperate and chronic viral lifestyles, we present model predictions using parameters taken from the human pathogens *P. aeruginosa* or *E. coli* and their viruses (see Table II). Besides their medical relevance, *P. aeruginosa* and *E. coli* are among the most well-studied microbes in science. We initialize the system with $S(0) = 1\text{e-}3$, $V_T(0) = V_C(0) = 1\text{e-}7$ and all others zero, following [26]; no bistability exists for our parameter values, so the initial condition does not affect the steady state (see Supplementary Information). Because we are primarily interested in recovery from infection that is passed vertically to daughter cells, we take $\gamma_I = 0$ for the remainder of the paper. The results are qualitatively similar for $\gamma_I > 0$; see Supplementary Information for full model analysis.

A. Model behavior

In Figure 2, we simulate the model system for the baseline parameter values in Table II. We see a rapid initial growth of the susceptible population followed quickly by a population crash caused primarily by lytic infection. Filling the niche created by the susceptible population crash are the latent lytic bacteria. After dozens of bacterial divisions, the latent lytic bacteria recover from infection create a niche for chronically infected bacteria. Eventually, the chronically infected bacteria become the most abundant in the system because chronic viruses do not require new susceptible bacteria in order to reproduce.

Although chronically infected bacteria dominate the system, free temperate viruses stabilize at over twice the density of free chronic viruses (Figure 2b). Although little is known about the proportion of each viral type seen in natural environments, it is known that temperate and chronic viruses frequently coexist [56]. The model predicts that the total virus to total bacteria ratio stabilizes at 58:1, which falls within the typical range of virus to bacteria ratios seen in natural environments [57, 58].

The model behaviors presented here use the baselines in Table II. However, the equilibria and their respective stability depends on nearly all the model parameters (see the Supplementary Information for more details).

B. Steady states and stability

While many evolvable parameters (such as viral burst sizes and bacterial growth rates) are likely limited by physical constraints, lysogen frequency could theoretically take on any value. Lysogen frequency is of particular interest because latency involves inherent tradeoffs between vertical and horizontal transmission; the lytic strategy relies on horizontal transmission only, while the latent strategy uses only vertical transmission.

Therefore, our primary interest for this study is the lysogen frequencies for temperate and chronic viruses; we look at the possible steady state outcomes for all possible combinations of lysogen frequencies f_T and f_C with all other parameters held constant at the baselines in Table II. Only four stable steady states exist: **coexistence** (all populations exceed 0),

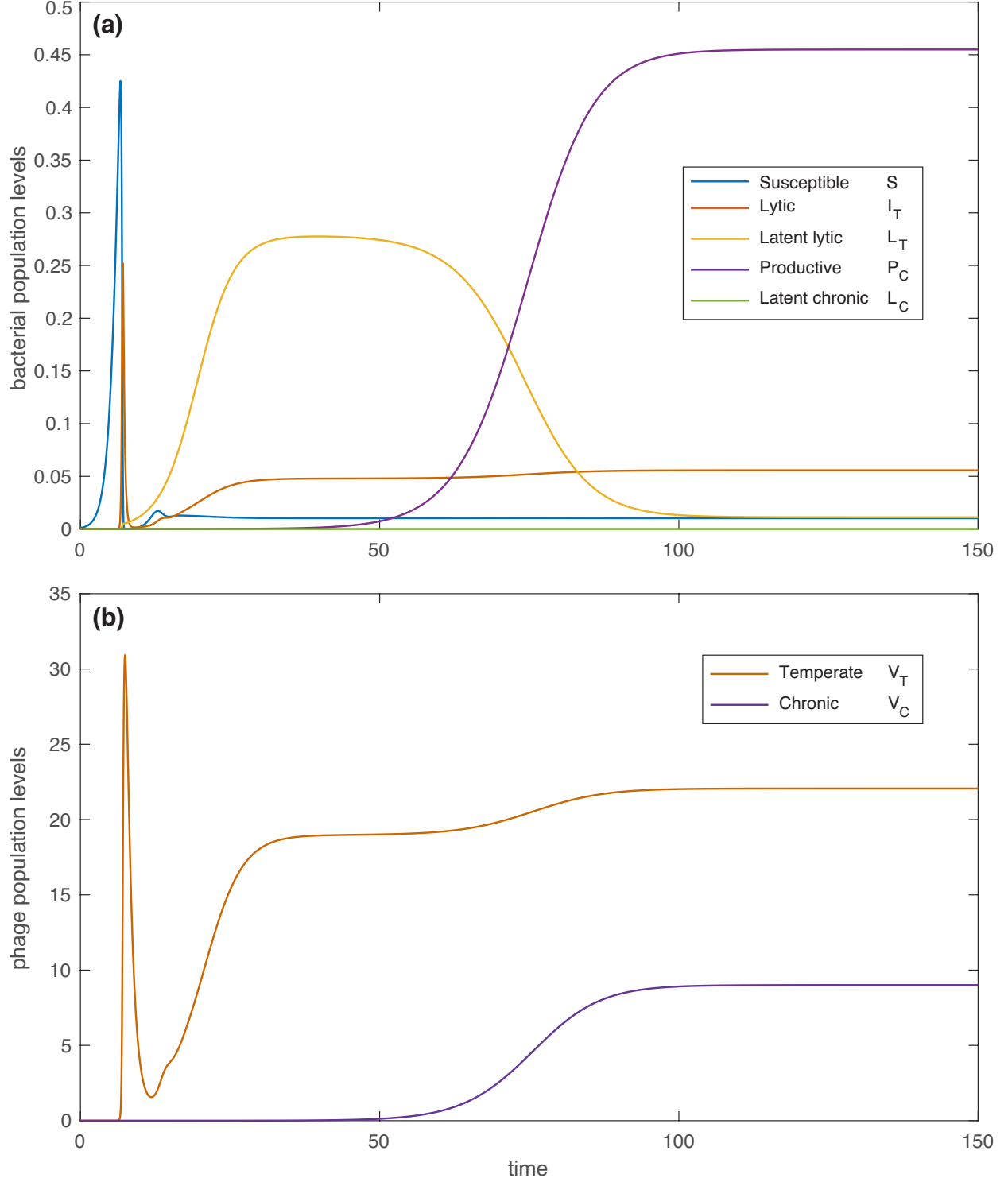


FIG. 2. Simulation of model equations (1-7). Initial conditions are $S(0) = 1e-3$, $V_T(0) = V_C(0) = 1e-7$ with all others zero. All parameters are held constant at the baseline values given in Table II. Eventually the temperate and chronic viral strategies reach a stable coexistence state.

temperate strategy only ($V_C = P_C = L_C = 0$), **chronic strategy only** ($V_T = I_T = L_T = 0$), and **susceptible only** (all populations, except S , are 0). See Figure 3 for the bifurcation diagram.

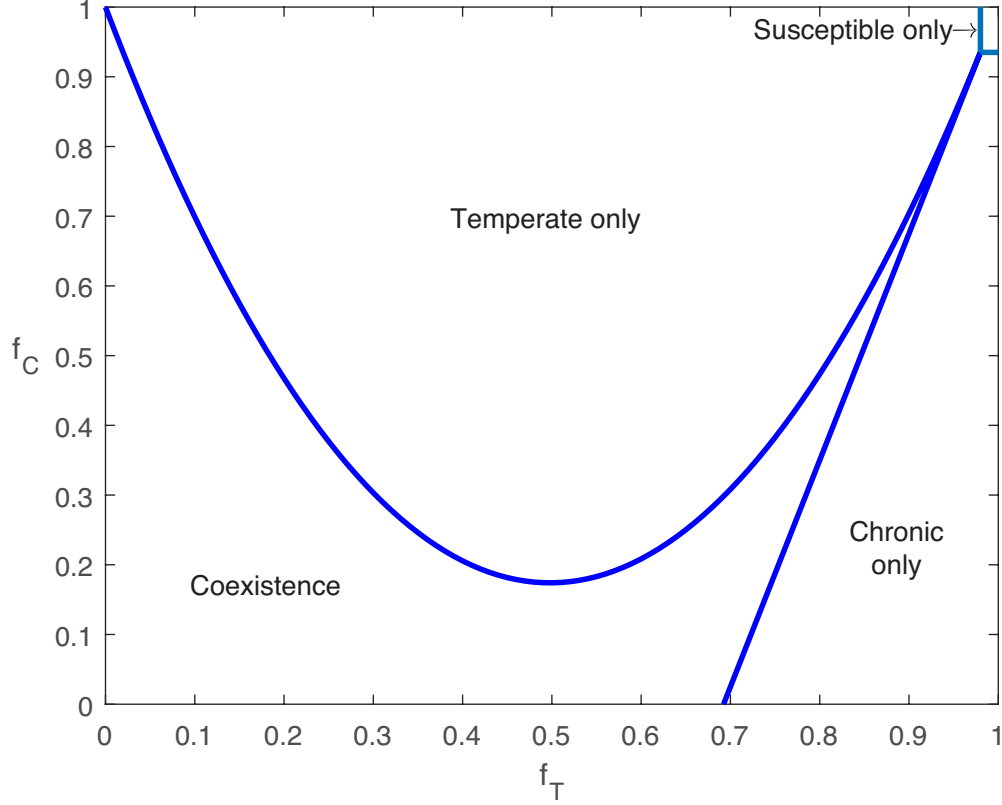


FIG. 3. Bifurcation diagram of lysogen frequencies for temperate and chronic viruses. Holding all other parameters constant at the baseline values given in Table II, we find that four steady state outcomes are possible: coexistence of both viral strategies, temperate survival with chronic extinction, chronic survival with temperate extinction, and extinction of both viral strategies (susceptible bacteria the only survivors). If the lysogen frequency for a particular viral type is too high, then that virus will not survive. If lysogen frequencies are low enough for both viral types, then the viruses will coexist. This bifurcation diagram was generated using standard linear stability analysis; see the Supplementary Information for details on the viral invasion analysis.

Temperate viruses can outcompete chronic viruses if the temperate lysogen frequency is neither too large nor too small (see ‘Temperate only’ region of Figure 3). If the temperate lysogen frequency is too high, then chronic viruses will be produced in large numbers relative to temperate; chronic viruses will infect susceptible bacteria first, eventually driving temperate viruses to extinction (see ‘Chronic only’ region of Figure 3). If the temperate lysogen frequency is too low, then temperate viruses lyse bacteria too quickly, leaving room for productive bacteria to reproduce while the susceptible population also grows; if the productive bacterial population is large enough (i.e., chronic lysogen frequencies are sufficiently low), then both viral types will coexist (see ‘Coexistence’ region of Figure 3). See the Supplementary Information for the complete steady state analysis.

C. Temperate viruses exhibit a ‘sweet spot’ lysogen frequency

Temperate viruses are known to exhibit a small, nonzero lysogen frequency [1, 29, 30, 46–52]. Our model illustrates why temperate viruses have a theoretical ‘sweet spot’ lysogen frequency when competing with chronic viruses.

Suppose that temperate viruses select¹ a lysogen frequency f_T that maximizes steady state viral abundance, including both free viruses (V_T) and proviruses (L_T , as proxy). Because chronic viruses may also select a lysogen frequency f_C that maximizes their viral density, the optimal lysogen frequency for temperate viruses depends on f_C .

Figure 4(a) shows the steady state temperate viral density for all possible combinations of f_T and f_C . Given any chronic lysogen frequency f_C , temperate viruses may select a lysogen frequency f_T that conditionally maximizes their viral density (optimal strategies are shown in red). We see that for all possible chronic latency strategies, there exists a small but nonzero (i.e., sweet spot) lysogen frequency f_T that maximizes temperate viral density at steady state.

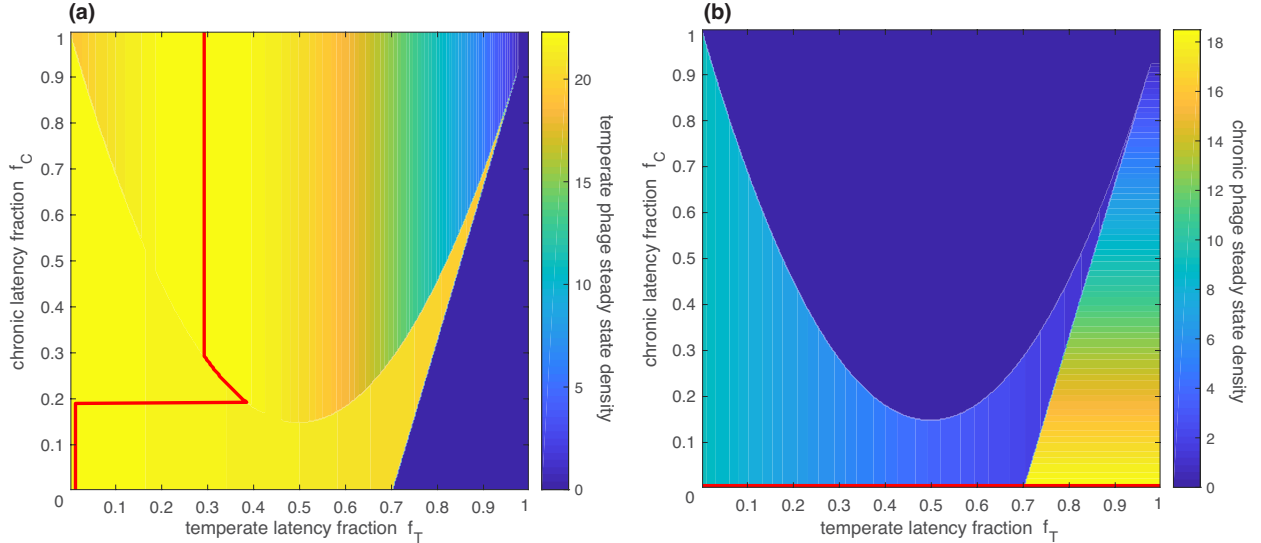


FIG. 4. Viral steady state density over the full range of possible lysogen frequencies ($0 \leq f_i \leq 1$) for temperate and chronic viruses. Color indicates the steady state viral density, and the red line is the maximum steady state density for each lysogen frequency of the competing virus. **(a)** Temperate virus density ($V_T + L_T$) at steady state. The red curve shows the maximum steady state density for every possible chronic lysogen frequency. Note that the optimal temperate lysogen frequency jumps from nearly 40% lysogeny to about 1% lysogeny when the chronic lysogen frequency drops below 20%. This rapid transition occurs because the optimal state for the temperate virus jumps from a temperate only state to a coexistence steady state. **(b)** Chronic virus density ($V_C + L_C$) at steady state. The red curve shows that the maximum steady state density for every possible chronic lysogen frequency is $f_C = 0$. Taking these two steady state density profiles together, it is evident that chronic viruses should avoid latency ($f_C = 0$), and therefore temperate viruses should adopt a lysogen frequency near $f_T = 0.01$.

¹ We use ‘select’ in the sense of evolutionary game theory.

D. Chronic viruses should eliminate latency

While lysogen frequencies for temperate viruses are well-studied, lysogen frequencies for chronic viruses are unknown. Our model reveals that the lysogen frequency for chronic viruses should be exactly zero. In Figure 4(b), we plot the steady state density of chronic viruses in the system ($V_C + L_C$). For any given temperate viral lysogen frequency f_T , chronic viruses maximize steady state density by selecting a lysogen frequency $f_C = 0$. From an ecological perspective, this result is intuitive. We have assumed that there is no reproductive cost to productive infection relative to latent infection, so it benefits chronic viruses to spread genetic material both horizontally (via production) and vertically (via cell division), rather than vertically alone.

E. Bacterial recovery rate determinable using viral abundance

We use our conclusion that $f_C = 0$, along with the fact that temperate viruses possess a lysogen frequency around 1% to deduce the typical bacterial recovery (cure) rates. In the interest of simplicity, we assume all recovery rates are equal: $\gamma = \gamma_T = \gamma_P = \gamma_C$. The appropriate recovery rates should lead to a maximum temperate virus steady state density ($V_T + L_T$) for $f_C = 0$ and $f_T \approx 0.01$, which occurs over only a small range of $\gamma \approx 0.67$; see Figure 4(a).

A wide range of outcomes is possible if the recovery rate γ is not near 0.67 (see Figure 5), but none include temperate lysogen frequencies near 1% and coexistence of both viral types, as we see in many natural environments.

For $\gamma \leq 0.2$ (very slow intracellular provirus deactivation), optimal temperate lysogen frequencies are $f_T = 0$ when chronic viruses select the optimal lysogen frequency of $f_C = 0$ (see Figure 5). However, temperate viruses are effectively driven to extinction under these conditions, implying that extremely stable proviruses are deleterious to temperate viruses. Due to the presence of both viral types in many environments, we suspect that intracellular provirus deactivation is not extremely slow.

For moderately slow intracellular provirus deactivation ($0.22 \leq \gamma \leq 0.66$), optimal temperate lysogen frequencies exceed 5% (see Figure 5). This result implies that temperate viruses more resilient to deactivation should also increase latency.

If instead $0.68 \leq \gamma \leq 0.79$ (moderately fast intracellular provirus deactivation), then the optimal temperate lysogen frequency is exactly zero again (see Figure 5). In other words, for faster recovery rates, all temperate viruses would be obligately lytic. Due to this result, we speculate that temperate proviruses are more resilient to intracellular deactivation than obligately lytic viruses.

For $\gamma \geq 0.8$ (very fast intracellular deactivation), lysogen frequencies instantaneously jump to around $f_T = 0.5$, and chronic viruses are driven to extinction (see Figure 5).

IV. DISCUSSION

A. Recovery rates and lysogen frequencies

In environments where temperate and chronic viruses coexist, bacterial recovery rates should be near $\gamma = 0.67$. If proviruses are slightly more stable, then we would expect

to see higher lysogen frequencies for temperate viruses. For proviruses that are stable on evolutionary timescales, we would expect to see chronic viruses dominate. For proviruses that are slightly less stable, we would expect to see the latency strategy disappear. For proviruses that are quickly deactivated, we would expect to see temperate viruses dominate with large lysogen frequencies. This predicted recovery rate is faster than one might expect, so we hope this study encourages more experimental work on the intracellular deactivation of proviruses within *P. aeruginosa*.

B. Limitations

With the goal of keeping the model analytically tractable, we have made simplifying assumptions that may affect the presented results. First, we have assumed mass action infection dynamics, but *P. aeruginosa*-virus infection rates may not be well-approximated by a mass action process, especially for large bacteria population sizes [59, 60]. More realistically, infection rates may slow as population growth activates quorum-sensing and biofilm formation [53].

In addition, we have assumed the lytic recovery rate is zero and all other recovery rates are equal. Although assuming $\gamma_I = 0$ produces qualitatively similar results to $\gamma_I = \gamma_T$, it may not be reasonable to assume that all other recovery rates are equal. Future study is needed to determine how recovery rates are affected by the infection type.

We have also assumed that both viral types produce super-infection and cross-infection exclusion proteins that prevent a second infection of any kind. While many viruses that infect *P. aeruginosa* produce super-infection exclusion proteins that effectively prevent multiple infections by the same viral type [61, 62], little is known about cross resistance to viral infection.

Another simplifying assumption is that lysogen frequencies are constant, but some viruses are able to detect bacteria population density, which appears to affect the frequency of lysogeny [54, 55]. If this process applies to *P. aeruginosa* and its viruses, a more sophisticated model would incorporate a density-dependent latency probability: $f_T(N)$ and $f_C(N)$.

Finally, in deducing the expected chronic lysogen frequency f_C and the recovery (cure) rates γ , we have assumed that all other parameters are exactly the baselines given in Table II. While the literature has provided reasonable ranges for these parameters, several baseline values (e.g., β_C , η_T , and η_C) were simply selected within those ranges. Given the uncertainty in several parameter values, the model-inferred parameters f_C and γ are also uncertain.

C. Future steps

This model could serve as a base for more sophisticated extensions. For instance, the presented model does not include an evolutionary component and is therefore only applicable on short time scales. However, this model could be part of a multi-scale model that incorporates both short time-scale (ecological) dynamics and long time-scale (evolutionary) dynamics.

Also, we have assumed that no environmental stressors (e.g., radiation, heat, sublethal antibiotics) perturb the system, but antibiotics are often used to treat bacterial infections. Many classes of antibiotics are known to induce latent proviruses and trigger virus production, even if the bacteria are antibiotic resistant [63–67]. In fact, the induction of latent

viruses is proposed to be one of the mechanisms behind the synergistic effect of antibiotics and viruses to treat recalcitrant bacterial infections [67, 68]. Infections by *P. aeruginosa* represent about 10% of nosocomial infections, are a leading cause of death among patients with cystic fibrosis, and have been deemed a serious threat on the United States Centers for Disease Control watch list for antibiotic resistance [15–17]; therefore, a critical next step is understanding the impact of antibiotic-induced proviruses on control of bacterial infections. This is the subject of ongoing study.

V. CONCLUSION

We have developed a simple mathematical model of the ecological competition between temperate and chronic viruses for bacterial hosts. Using the hosts *E. coli* and *P. aeruginosa* as motivation, we demonstrate that low lysogen frequencies provide competitive advantages for both viral types. Interestingly, chronic viruses theoretically maximize their steady state density by eliminating latency entirely, but temperate viruses exhibit a non-zero ‘sweet spot’ lysogen frequency. Using experimental evidence that temperate viruses possess lysogen frequencies around 1% and that both viral types coexist in real environments, we are able to estimate the recovery (cure) rates for bacteria. Better understanding of this system may contribute to optimal treatment of bacterial infections using phage therapy and/or antibiotics.

VI. ACKNOWLEDGEMENTS

This work was funded in part by the National Science Foundation grant DMS-1815764 (ZR), the Cystic Fibrosis Foundation grant WHITAK16PO (RJW), and an Allen Distinguished Investigator Award (RJW). The funders had no role in study design, data collection and analysis, decision to publish, or preparation of the manuscript.

The authors thank Jayadevi H. Chandrashekhar, Ted Kim, and George A. O’Toole for discussions that informed biological aspects of this work.

VII. DATA AVAILABILITY

All software (Matlab .m files) will be made publicly available via the Illinois Data Bank pending publication in a peer-reviewed journal.

VIII. COMPETING INTERESTS

The authors declare no competing interests.

-
- [1] R. Calendar, *The bacteriophages*. Oxford University Press on Demand, 2006.
 - [2] N. J. Dimmock, A. J. Easton, and K. N. Leppard, *Introduction to modern virology*. John Wiley & Sons, 2016.

- [3] M. G. Weinbauer, "Ecology of prokaryotic viruses," *FEMS microbiology reviews*, vol. 28, no. 2, pp. 127–181, 2004.
- [4] J. Rakonjac, *Filamentous Bacteriophages: Biology and Applications*. American Cancer Society, 2012.
- [5] A. Lwoff, "Lysogeny," *Bacteriological Reviews*, vol. 17, no. 4, p. 269, 1953.
- [6] E. V. Davies, C. Winstanley, J. L. Fothergill, and C. E. James, "The role of temperate bacteriophages in bacterial infection," *FEMS microbiology letters*, vol. 363, no. 5, 2016.
- [7] S. Roux, S. J. Hallam, T. Woyke, and M. B. Sullivan, "Viral dark matter and virus–host interactions resolved from publicly available microbial genomes," *Elife*, vol. 4, p. e08490, 2015.
- [8] K. Mathee, G. Narasimhan, C. Valdes, X. Qiu, J. M. Matewish, M. Koehrsen, A. Rokas, C. N. Yandava, R. Engels, E. Zeng, *et al.*, "Dynamics of pseudomonas aeruginosa genome evolution," *Proceedings of the National Academy of Sciences*, vol. 105, no. 8, pp. 3100–3105, 2008.
- [9] J. Mosquera-Rendón, A. M. Rada-Bravo, S. Cárdenas-Brito, M. Corredor, E. Restrepo-Pineda, and A. Benítez-Páez, "Pangenome-wide and molecular evolution analyses of the pseudomonas aeruginosa species," *BMC genomics*, vol. 17, no. 1, p. 45, 2016.
- [10] D. H. Spencer, A. Kas, E. E. Smith, C. K. Raymond, E. H. Sims, M. Hastings, J. L. Burns, R. Kaul, and M. V. Olson, "Whole-genome sequence variation among multiple isolates of pseudomonas aeruginosa," *Journal of bacteriology*, vol. 185, no. 4, pp. 1316–1325, 2003.
- [11] V. L. Kung, E. A. Ozer, and A. R. Hauser, "The accessory genome of pseudomonas aeruginosa," *Microbiology and molecular biology reviews*, vol. 74, no. 4, pp. 621–641, 2010.
- [12] J. Courtney, J. Bradley, J. McCaughan, T. O’connor, C. Shortt, C. Bredin, I. Bradbury, and J. Elborn, "Predictors of mortality in adults with cystic fibrosis," *Pediatric pulmonology*, vol. 42, no. 6, pp. 525–532, 2007.
- [13] J. Emerson, M. Rosenfeld, S. McNamara, B. Ramsey, and R. L. Gibson, "Pseudomonas aeruginosa and other predictors of mortality and morbidity in young children with cystic fibrosis," *Pediatric pulmonology*, vol. 34, no. 2, pp. 91–100, 2002.
- [14] G. M. Nixon, D. S. Armstrong, R. Carzino, J. B. Carlin, A. Olinsky, C. F. Robertson, and K. Grimwood, "Clinical outcome after early pseudomonas aeruginosa infection in cystic fibrosis," *The Journal of pediatrics*, vol. 138, no. 5, pp. 699–704, 2001.
- [15] W. R. Jarvis and W. J. Martone, "Predominant pathogens in hospital infections," *Journal of Antimicrobial Chemotherapy*, vol. 29, no. suppl_A, pp. 19–24, 1992.
- [16] R. E. Hancock and D. P. Speert, "Antibiotic resistance in pseudomonas aeruginosa: mechanisms and impact on treatment," *Drug resistance updates*, vol. 3, no. 4, pp. 247–255, 2000.
- [17] US Department of Health and Human Services, "Antibiotic resistance threats in the united states, 2013," *Centers for Disease Control and Prevention*, 2013.
- [18] F. L. G. Altamirano and J. J. Barr, "Phage therapy in the postantibiotic era," *Clinical microbiology reviews*, vol. 32, no. 2, pp. e00066–18, 2019.
- [19] A. Sulakvelidze, Z. Alavidze, and J. G. Morris, "Bacteriophage therapy," *Antimicrobial agents and chemotherapy*, vol. 45, no. 3, pp. 649–659, 2001.
- [20] Y. Lin, R. Y. K. Chang, W. J. Britton, S. Morales, E. Kutter, and H.-K. Chan, "Synergy of nebulized phage pev20 and ciprofloxacin combination against pseudomonas aeruginosa," *International journal of pharmaceuticals*, vol. 551, no. 1-2, pp. 158–165, 2018.
- [21] A. M. Comeau, F. Tétart, S. N. Trojet, M.-F. Prere, and H. Krisch, "Phage-antibiotic synergy (pas): β -lactam and quinolone antibiotics stimulate virulent phage growth," *PLoS One*, vol. 2,

- no. 8, p. e799, 2007.
- [22] E. Kutter, D. De Vos, G. Gvasalia, Z. Alavidze, L. Gogokhia, S. Kuhl, and S. T. Abedon, “Phage therapy in clinical practice: treatment of human infections,” *Current pharmaceutical biotechnology*, vol. 11, no. 1, pp. 69–86, 2010.
 - [23] S. Clifton, T. Kim, J. H. Chandrashekhar, G. A. O’Toole, Z. Rapti, and R. J. Whitaker, “Modeling the control of bacterial infections via antibiotic-induced proviruses,” *bioRxiv*, p. 706796, 2019.
 - [24] J. S. Weitz and J. Dushoff, “Alternative stable states in host–phage dynamics,” *Theoretical Ecology*, vol. 1, no. 1, pp. 13–19, 2008.
 - [25] R. J. Payne and V. A. Jansen, “Understanding bacteriophage therapy as a density-dependent kinetic process,” *Journal of Theoretical Biology*, vol. 208, no. 1, pp. 37–48, 2001.
 - [26] V. Sinha, A. Goyal, S. L. Senningsen, S. Semsey, and S. Krishna, “In silico evolution of lysis-lysogeny strategies reproduces observed lysogeny propensities in temperate bacteriophages,” *Frontiers in microbiology*, vol. 8, p. 1386, 2017.
 - [27] H. Gulbudak and J. S. Weitz, “Heterogeneous viral strategies promote coexistence in virus-microbe systems,” *Journal of theoretical biology*, vol. 462, pp. 65–84, 2019.
 - [28] J. S. Weitz, G. Li, H. Gulbudak, M. H. Cortez, and R. J. Whitaker, “Viral invasion fitness across a continuum from lysis to latency,” *Virus Evolution*, vol. 5, no. 1, p. vez006, 2019.
 - [29] A. B. Oppenheim, S. L. Adhya, *et al.*, “A new look at bacteriophage λ genetic networks,” *Journal of bacteriology*, vol. 189, no. 2, pp. 298–304, 2007.
 - [30] V. V. Volkova, Z. Lu, T. Besser, and Y. T. Gröhn, “Modeling the infection dynamics of bacteriophages in enteric escherichia coli: estimating the contribution of transduction to antimicrobial gene spread,” *Appl. Environ. Microbiol.*, vol. 80, no. 14, pp. 4350–4362, 2014.
 - [31] H. Brüssow, C. Canchaya, and W.-D. Hardt, “Phages and the evolution of bacterial pathogens: from genomic rearrangements to lysogenic conversion,” *Microbiol. Mol. Biol. Rev.*, vol. 68, no. 3, pp. 560–602, 2004.
 - [32] P. Horvath and R. Barrangou, “Crispr/cas, the immune system of bacteria and archaea,” *Science*, vol. 327, no. 5962, pp. 167–170, 2010.
 - [33] M. Zwietering, I. Jongenburger, F. Rombouts, and K. Van’t Riet, “Modeling of the bacterial growth curve,” *Applied and environmental microbiology*, vol. 56, no. 6, pp. 1875–1881, 1990.
 - [34] J. W. Shapiro, E. S. Williams, and P. E. Turner, “Evolution of parasitism and mutualism between filamentous phage m13 and escherichia coli,” *PeerJ*, vol. 4, p. e2060, 2016.
 - [35] A. Tabib-Salazar, B. Liu, A. Shadrin, L. Burchell, Z. Wang, Z. Wang, M. G. Goren, I. Yosef, U. Qimron, K. Severinov, *et al.*, “Full shut-off of escherichia coli rna-polymerase by t7 phage requires a small phage-encoded dna-binding protein,” *Nucleic acids research*, vol. 45, no. 13, pp. 7697–7707, 2017.
 - [36] F. St-Pierre and D. Endy, “Determination of cell fate selection during phage lambda infection,” *Proceedings of the National Academy of Sciences*, vol. 105, no. 52, pp. 20705–20710, 2008.
 - [37] A. M. Nanda, K. Thormann, and J. Frunzke, “Impact of spontaneous prophage induction on the fitness of bacterial populations and host-microbe interactions,” *Journal of bacteriology*, vol. 197, no. 3, pp. 410–419, 2015.
 - [38] A. J. Garro and M.-F. Law, “Relationship between lysogeny, spontaneous induction, and transformation efficiencies in bacillus subtilis,” *Journal of bacteriology*, vol. 120, no. 3, pp. 1256–1259, 1974.
 - [39] M. G. Cortes, J. Krog, and G. Balazsi, “Optimality of the spontaneous prophage induction rate,” *bioRxiv*, 2019.

- [40] S. Casjens, “Prophages and bacterial genomics: what have we learned so far?,” *Molecular microbiology*, vol. 49, no. 2, pp. 277–300, 2003.
- [41] Z. Hobbs and S. T. Abedon, “Diversity of phage infection types and associated terminology: the problem with lytic or lysogenic,” *FEMS microbiology letters*, vol. 363, no. 7, 2016.
- [42] J. De Smet, H. Hendrix, B. G. Blasdel, K. Danis-Wlodarczyk, and R. Lavigne, “Pseudomonas predators: Understanding and exploiting phage–host interactions,” *Nature Reviews Microbiology*, vol. 15, no. 9, p. 517, 2017.
- [43] M. Heldal and G. Bratbak, “Production and decay of viruses in aquatic environments,” *Marine Ecology Progress Series*, pp. 205–212, 1991.
- [44] C. Spalding, E. Keen, D. J. Smith, A.-M. Krachler, and S. Jabbari, “Mathematical modelling of the antibiotic-induced morphological transition of pseudomonas aeruginosa,” *PLoS computational biology*, vol. 14, no. 2, p. e1006012, 2018.
- [45] S. H. Kopf, A. L. Sessions, E. S. Cowley, C. Reyes, L. Van Sambeek, Y. Hu, V. J. Orphan, R. Kato, and D. K. Newman, “Trace incorporation of heavy water reveals slow and heterogeneous pathogen growth rates in cystic fibrosis sputum,” *Proceedings of the National Academy of Sciences*, vol. 113, no. 2, pp. E110–E116, 2016.
- [46] X. Yu, Y. Xu, Y. Gu, Y. Zhu, and X. Liu, “Characterization and genomic study of phikmv-like phage paxyb1 infecting pseudomonas aeruginosa,” *Scientific reports*, vol. 7, no. 1, p. 13068, 2017.
- [47] G. El Didamony, A. Askora, and A. A. Shehata, “Isolation and characterization of t7-like lytic bacteriophages infecting multidrug resistant pseudomonas aeruginosa isolated from egypt,” *Current microbiology*, vol. 70, no. 6, pp. 786–791, 2015.
- [48] L. Latino, C. Essoh, Y. Blouin, H. V. Thien, and C. Pourcel, “A novel pseudomonas aeruginosa bacteriophage, ab31, a chimera formed from temperate phage paju2 and p. putida lytic phage af: characteristics and mechanism of bacterial resistance,” *PloS one*, vol. 9, no. 4, p. e93777, 2014.
- [49] H. S. Schrader, J. O. Schrader, J. J. Walker, T. A. Wolf, K. W. Nickerson, and T. A. Kokjohn, “Bacteriophage infection and multiplication occur in pseudomonas aeruginosa starved for 5 years,” *Canadian journal of microbiology*, vol. 43, no. 12, pp. 1157–1163, 1997.
- [50] P.-J. Ceyssens, A. Brabban, L. Rogge, M. S. Lewis, D. Pickard, D. Goulding, G. Dougan, J.-P. Noben, A. Kropinski, E. Kutter, *et al.*, “Molecular and physiological analysis of three pseudomonas aeruginosa phages belonging to the n4-like viruses,” *Virology*, vol. 405, no. 1, pp. 26–30, 2010.
- [51] J. Garbe, B. Bunk, M. Rohde, and M. Schobert, “Sequencing and characterization of pseudomonas aeruginosa phage jg004,” *BMC microbiology*, vol. 11, no. 1, p. 102, 2011.
- [52] L. You, P. F. Suthers, and J. Yin, “Effects of escherichia coli physiology on growth of phage t7 in vivo and in silico,” *Journal of bacteriology*, vol. 184, no. 7, pp. 1888–1894, 2002.
- [53] D. R. Harper, H. M. Parracho, J. Walker, R. Sharp, G. Hughes, M. Werthén, S. Lehman, and S. Morales, “Bacteriophages and biofilms,” *Antibiotics*, vol. 3, no. 3, pp. 270–284, 2014.
- [54] K. R. Hargreaves, A. M. Kropinski, and M. R. Clokie, “What does the talking?: quorum sensing signalling genes discovered in a bacteriophage genome,” *PloS one*, vol. 9, no. 1, p. e85131, 2014.
- [55] J. E. Silpe and B. L. Bassler, “A host-produced quorum-sensing autoinducer controls a phage lysis-lysogeny decision,” *Cell*, 2018.
- [56] C. Winstanley, M. G. Langille, J. L. Fothergill, I. Kukavica-Ibrulj, C. Paradis-Bleau, F. Sanschagrin, N. R. Thomson, G. L. Winsor, M. A. Quail, N. Lennard, *et al.*, “Newly introduced

- genomic prophage islands are critical determinants of in vivo competitiveness in the liverpool epidemic strain of *pseudomonas aeruginosa*,” *Genome research*, vol. 19, no. 1, pp. 12–23, 2009.
- [57] C. E. James, E. V. Davies, J. L. Fothergill, M. J. Walshaw, C. M. Beale, M. A. Blockhurst, and C. Winstanley, “Lytic activity by temperate phages of *pseudomonas aeruginosa* in long-term cystic fibrosis chronic lung infections,” *The ISME Journal*, vol. 9, pp. 1391–1398, 2015.
 - [58] B. Knowles, C. Silveira, B. Bailey, K. Barott, V. Cantu, A. Cobián-Güemes, F. Coutinho, E. Dinsdale, B. Felts, K. Furby, *et al.*, “Lytic to temperate switching of viral communities,” *Nature*, vol. 531, no. 7595, p. 466, 2016.
 - [59] M. Simmons, K. Drescher, C. D. Nadell, and V. Bucci, “Phage mobility is a core determinant of phage–bacteria coexistence in biofilms,” *The ISME journal*, vol. 12, no. 2, p. 531, 2017.
 - [60] L. Vidakovic, P. K. Singh, R. Hartmann, C. D. Nadell, and K. Drescher, “Dynamic biofilm architecture confers individual and collective mechanisms of viral protection,” *Nature microbiology*, vol. 3, no. 1, p. 26, 2018.
 - [61] Y.-J. Heo, I.-Y. Chung, K. B. Choi, G. W. Lau, and Y.-H. Cho, “Genome sequence comparison and superinfection between two related *pseudomonas aeruginosa* phages, d3112 and mp22,” *Microbiology*, vol. 153, no. 9, pp. 2885–2895, 2007.
 - [62] C. E. James, J. L. Fothergill, H. Kalwij, A. J. Hall, J. Cottell, M. A. Brockhurst, and C. Winstanley, “Differential infection properties of three inducible prophages from an epidemic strain of *pseudomonas aeruginosa*,” *BMC microbiology*, vol. 12, no. 1, p. 216, 2012.
 - [63] A. Rokney, O. Kobiler, A. Amir, D. L. Court, J. Stavans, S. Adhya, and A. B. Oppenheim, “Host responses influence on the induction of lambda prophage,” *Molecular microbiology*, vol. 68, no. 1, pp. 29–36, 2008.
 - [64] J. L. Fothergill, E. Mowat, M. J. Walshaw, M. J. Ledson, C. E. James, and C. Winstanley, “Effect of antibiotic treatment on bacteriophage production by a cystic fibrosis epidemic strain of *pseudomonas aeruginosa*,” *Antimicrobial agents and chemotherapy*, vol. 55, no. 1, pp. 426–428, 2011.
 - [65] E. López, A. Domenech, M.-J. Ferrándiz, M. J. Frias, C. Ardanuy, M. Ramirez, E. García, J. Liñares, and G. Adela, “Induction of prophages by fluoroquinolones in *streptococcus pneumoniae*: implications for emergence of resistance in genetically-related clones,” *PloS one*, vol. 9, no. 4, p. e94358, 2014.
 - [66] E. Martínez-García, T. Jatsenko, M. Kivisaar, and V. de Lorenzo, “Freeing *pseudomonas putida* kt 2440 of its proviral load strengthens endurance to environmental stresses,” *Environmental microbiology*, vol. 17, no. 1, pp. 76–90, 2015.
 - [67] S. Kaur, K. Harjai, and S. Chhibber, “Plaque-size enhancement of mrsa phages using sublethal concentrations of antibiotics,” *Applied and environmental microbiology*, pp. AEM–02371, 2012.
 - [68] M. Kim, Y. Jo, Y. J. Hwang, H. W. Hong, S. S. Hong, K. Park, and H. Myung, “Phage-antibiotic synergy via delayed lysis,” *Appl. Environ. Microbiol.*, vol. 84, no. 22, pp. e02085–18, 2018.
 - [69] O. Diekmann, J. Heesterbeek, and J. Metz, “On the definition and the computation of the basic reproduction ratio r_0 in models of infectious diseases in heterogeneous population,” *Journal of Mathematical Biology*, vol. 28, pp. 365–382, 1990.
 - [70] Z. Rapti and C. Cáceres, “Effects of intrinsic and extrinsic host mortality on disease spread,” *Bulletin of Mathematical Biology*, vol. 78, pp. 235–253, 2016.
 - [71] V. Andreasen and A. Pugliese, “Pathogen coexistence induced by density-dependent host mortality,” *Journal of theoretical biology*, vol. 177, no. 2, pp. 159–165, 1995.

- [72] B. Adams and A. Sasaki, “Cross-immunity, invasion and coexistence of pathogen strains in epidemiological models with one-dimensional antigenic space,” *Mathematical Biosciences*, vol. 210, no. 2, pp. 680–699, 2007.
- [73] E. Beretta and Y. Kuang, “Modeling and analysis of a marine bacteriophage infection,” *Mathematical Biosciences*, vol. 149, pp. 57–76, 1998.
- [74] M. A. Gilchrist, D. Sulsky, and A. Pringle, “Identifying fitness and optimal life-history strategies for an asexual filamentous fungus,” *Evolution*, vol. 60, pp. 970–979, 2006.
- [75] R. J. H. Payne and V. A. A. Jansen, “Pharmacokinetic principles of bacteriophage therapy,” *Clinical Pharmacokinetics*, vol. 42, pp. 315–325, 2003.
- [76] L. M. Wahl, M. I. Betti, D. W. Dick, T. Pattenden, and A. J. Puccini, “Evolutionary stability of the lysis-lysogeny decision: Why be virulent?,” *Evolution*, vol. 73, no. 1, pp. 92–98, 2019.
- [77] T. F. Thingstad, S. Våge, J. E. Storesund, R.-A. Sandaa, and J. Giske, “A theoretical analysis of how strain-specific viruses can control microbial species diversity,” *Proceedings of the National Academy of Sciences*, vol. 111, no. 21, pp. 7813–7818, 2014.
- [78] F. A. Stressmann, G. B. Rogers, P. Marsh, A. K. Lilley, T. W. Daniels, M. P. Carroll, L. R. Hoffman, G. Jones, C. E. Allen, N. Patel, N. Forbes, B. Forbes, A. Tuck, and K. D. Bruce, “Does bacterial density in cystic fibrosis sputum increase prior to pulmonary exacerbation?,” *Journal of Cystic Fibrosis*, vol. 10, no. 5, pp. 357–365, 2011.
- [79] G. S. Stent *et al.*, “Molecular biology of bacterial viruses.,” *Molecular biology of bacterial viruses.*, 1963.
- [80] J. J. Barr, R. Auro, N. Sam-Soon, S. Kassegne, G. Peters, N. Bonilla, M. Hatay, S. Mourtada, B. Bailey, M. Youle, *et al.*, “Subdiffusive motion of bacteriophage in mucosal surfaces increases the frequency of bacterial encounters,” *Proceedings of the National Academy of Sciences*, vol. 112, no. 44, pp. 13675–13680, 2015.

S1. SUPPLEMENTARY INFORMATION

A. Steady states

The following biologically relevant steady-states exist for system (1-7).

- First, it can be readily seen that the trivial steady state, where all population densities are zero, exists.
- Second, the steady state where only the susceptible class persists and is equal to the bacterial carrying capacity, $S = K$, also exists for all parameter values.
- The steady state where only the temperate phage persists, namely $P_C = V_C = L_C = 0$, also exists. In this case it holds:

$$\begin{aligned}
 S &= \frac{\mu_T}{\eta_T} \frac{\delta + \gamma_I}{\beta_T \delta (1 - f_T) - (\delta + \gamma_I)} \\
 V_T &= \frac{\beta_T \delta (1 - f_T) - (\delta + \gamma_I)}{\mu_T (1 - f_T)} I_T \\
 I_T &= \frac{r_S S (K - S) (1 - f_T)}{(r_S S - \gamma_I K) (1 - f_T) + (\delta + \gamma_I) K} + \frac{(1 - f_T) (\gamma_T K - r_S S)}{(r_S S - \gamma_I K) (1 - f_T) + (\delta + \gamma_I) K} L_T \\
 r_T ((\gamma_T - \gamma_I) (1 - f_T) + \delta + \gamma_I) L_T^2 + (\gamma_T (1 - f_T) (r_S S + \delta K) + (\delta + \gamma_I) r_S f_T S - (\delta + f_T \gamma_I) r_T (K - S)) L_T - \\
 f_T (\delta + \gamma_I) r_S S (K - S) &= 0
 \end{aligned}$$

- Similarly, when only the chronic phage persists, namely when $I_T = V_T = L_T = 0$, it holds

$$\begin{aligned}
 S &= \frac{\mu_C}{\eta_C} \frac{\gamma_P}{\beta_C (1 - f_C) - \gamma_P} \\
 P_C &= \frac{K - S}{1 + \frac{f_C \gamma_P}{(1 - f_C) \gamma_C}} \\
 L_C &= \frac{f_C \gamma_P}{(1 - f_C) \gamma_C} P_C \\
 V_C &= \frac{\beta_C (1 - f_C) - \gamma_P}{\mu_C (1 - f_C)} P_C
 \end{aligned}$$

- Finally, if all population densities are positive, it holds

$$\begin{aligned}
 S &= \frac{\mu_T}{\eta_T} \frac{\delta + \gamma_I}{\beta_T \delta (1 - f_T) - (\delta + \gamma_I)} \\
 1 - \frac{N}{K} &= \frac{\gamma_P}{r_P} - \frac{(1 - f_C) \beta_C}{r_P} \frac{\eta_C S}{\eta_C S + \mu_C} \\
 V_T &= \frac{\beta_T \delta (1 - f_T) - (\delta + \gamma_I)}{\mu_T (1 - f_T)} I_T \\
 V_C &= \frac{\beta_C}{\eta_C S + \mu_C} P_C \\
 L_T &= \frac{f_T}{1 - f_T} \frac{\delta + \gamma_I}{\gamma_T - r_T (1 - \frac{N}{K})} I_T \\
 L_C &= \frac{\eta_C f_C \beta_C S}{\eta_C S + \mu_C} \frac{1}{\gamma_C - r_C (1 - \frac{N}{K})} P_C.
 \end{aligned}$$

The following linear 2×2 system can be solved to yield a unique steady-state.

$$\begin{aligned} & \left(\frac{\delta + \gamma_I}{1 - f_T} \frac{\gamma_T(1 - f_T) - r_T(1 - \frac{N}{K})}{\gamma_T - r_T(1 - \frac{N}{K})} - \gamma_I \right) I_T + \left(\frac{\eta_C \beta_C S}{\eta_C S + \mu_C} \frac{\gamma_C(1 - f_C) - r_C(1 - \frac{N}{K})}{\gamma_C - r_C(1 - \frac{N}{K})} - \gamma_P \right) P_C = \\ & r_S S \left(1 - \frac{N}{K} \right) \\ & \left(1 + \frac{f_T}{1 - f_T} \frac{\delta + \gamma_I}{\gamma_T - r_T(1 - \frac{N}{K})} \right) I_T + \left(1 + \frac{\eta_C f_C \beta_C S}{\eta_C S + \mu_C} \frac{1}{\gamma_C - r_C(1 - \frac{N}{K})} \right) P_C = N - S \end{aligned}$$

B. Viral invasion fitness

The basic reproductive number R_0 , traditionally defined as the average number of new infections generated by an infectious individual in an entirely susceptible population [69], has long been used to characterize a pathogen's fitness [28, 70–72]. The basic reproductive number has been found to be correlated with the between-host transmission rate [73], the number of free infective propagules produced per infected host (virions, in our case), and life-history traits such as mortality, fecundity, and growth [70, 74].

In this study, R_0 is used to determine the growth rate of a viral invader in a population of residents at steady state. Specifically, when either the temperate or chronic virus attempts to invade the bacterial population, the virus is successful when its respective R_0 is greater than one. Similarly, when one of the two viruses is the resident, the other virus can invade and coexist as long as its R_0 is greater than one. The various regions where each virus invades and persists are shown in Figure 3.

One of the goals and challenges of phage therapy is to ensure that there is active viral replication [25]. This occurs when, after an initial dose of the virus, it is able to proliferate in its bacterial host. There are cases however, when viral replication does not take place, so repeated administration of the virus is required. There already exist various models that study viral kinetics and provide thresholds that guarantee active replication of lytic-only viruses [25, 75]. Yet, as in most models, recovery of the bacterial host is neglected.

Given the large range of recovery rates that viruses exhibit [31, 32], in this work, we investigate and identify viral recovery strategies that optimize viral abundance. Although the basic reproductive number is a traditional measure of fitness (see e.g., [76]), using abundance as a proxy for competitive advantage is also common (see e.g., [77]).

C. Linear stability analysis and bifurcations

1. The trivial equilibrium is linearly unstable for all choices of parameter values.
2. The steady-state with $S = K$ is linearly stable as long as

$$R_T = \frac{(1 - f_T)\eta_T\beta_T\delta K}{(\mu_T + \eta_T K)(\delta + \gamma_I)} < 1, \quad R_C = \frac{(1 - f_C)\eta_C\beta_C K}{\gamma_P(\mu_C + \eta_C K)} < 1.$$

We notice from the previous section that when $S = K$ it holds

$$S = \frac{\mu_T}{\eta_T} \frac{\delta + \gamma_I}{\beta_T\delta(1 - f_T) - (\delta + \gamma_I)} = K \Leftrightarrow R_T = 1$$

and

$$S = \frac{\mu_C}{\eta_C} \frac{\gamma_P}{\beta_C(1 - f_C) - \gamma_P} = K \Leftrightarrow R_C = 1.$$

Therefore, the bacterium only ($S = K$) steady-state undergoes a transcritical bifurcation with the $P_C = V_C = L_C = 0$ (temperate only) steady state when $R_T = 1$. Similarly, it undergoes a transcritical bifurcation with the $I_T = V_T = L_T = 0$ (chronic only) steady state when $R_C = 1$.

3. The temperate only steady state undergoes a transcritical bifurcation with the coexistence steady state when

$$R_{TC} = \frac{(1 - f_C)\beta_C\eta_C S}{\eta_C S + \mu_C} \frac{1}{\gamma_P - r_P \left(1 - \frac{N}{K}\right)} = 1, \quad \text{where} \quad S = \frac{\mu_T}{\eta_T} \frac{\delta + \gamma_I}{\beta_T \delta (1 - f_T) - (\delta + \gamma_I)},$$

and $N = S + I_T + L_T$.

4. There is a transcritical bifurcation from the chronic only to the coexistence steady-state when

$$R_{CT} = \frac{(1 - f_T)\beta_T\delta\eta_T S}{(\eta_T S + \mu_T)(\delta + \gamma_I)} = 1, \quad \text{where} \quad S = \frac{\mu_C}{\eta_C} \frac{\gamma_P}{\beta_C(1 - f_C) - \gamma_P}.$$

All these bifurcations are obtained by a standard linear stability analysis around the relevant steady states.

D. Model non-dimensionalization

The model system (1-7) can be non-dimensionalized so that time and bacterial density are unitless quantities. We will illustrate with equation (1) with $\gamma_I = 0$, but the methodology is analogous for all other equations in the system. Suppose the system (1-7) has bacterial density units of CFU/mL and time units of minutes. Then equation (1) has units CFU/mL/min:

$$\frac{dS}{dt} = \underbrace{r_S S \left(1 - \frac{N}{K}\right)}_{\text{growth}} - \underbrace{\eta_T S V_T - \eta_C S V_C}_{\text{infection}} + \underbrace{\gamma_T L_T + \gamma_P P_C + \gamma_C L_C}_{\text{recovery}}.$$

We will divide the entire equation by $r_S K$, i.e. the bacterial growth rate (in min^{-1}) multiplied by the carrying capacity (in CFU/mL):

$$\frac{d(S/K)}{d(r_S t)} = \underbrace{\frac{S}{K} \left(1 - \frac{N}{K}\right)}_{\text{growth}} - \underbrace{\frac{\eta_T}{r_S} \frac{S}{K} V_T - \frac{\eta_C}{r_S} \frac{S}{K} V_C}_{\text{infection}} + \underbrace{\frac{\gamma_T}{r_S} \frac{L_T}{K} + \frac{\gamma_P}{r_S} \frac{P_C}{K} + \frac{\gamma_C}{r_S} \frac{L_C}{K}}_{\text{recovery}}.$$

Now $\tilde{S} = S/K$ is a unitless bacterial density, $\tilde{t} = r_S t$ is a unitless time, $\tilde{\eta}_i = \eta_i/r_S$ is an infection rate per PFU/mL, and $\tilde{\gamma}_i = \gamma_i/r_S$ is a unitless recovery rate:

$$\frac{d\tilde{S}}{d\tilde{t}} = \underbrace{\tilde{S} \left(1 - \tilde{N}\right)}_{\text{growth}} - \underbrace{\tilde{\eta}_T \tilde{S} V_T - \tilde{\eta}_C \tilde{S} V_C}_{\text{infection}} + \underbrace{\tilde{\gamma}_T \tilde{L}_T + \tilde{\gamma}_P \tilde{P}_C + \tilde{\gamma}_C \tilde{L}_C}_{\text{recovery}}.$$

For the sake of clarity, we have suppressed tilde notation throughout the main manuscript. The same effect is achieved by choosing $\gamma = 1$ and $K = 1$ in system (1-7) and reinterpreting bacterial populations as fractions of the carrying capacity and rates (except infection and adsorption) as multiples of the growth rate. All parameters in Table II have been scaled as such (details follow).

E. Parameter selection

The **growth rate** r_S for *P. aeruginosa in vitro* is approximately $5.1\text{e-}3 \text{ min}^{-1}$ [44], although *P. aeruginosa* growth is highly variable in humans [45]. Therefore all rate parameters provided in min^{-1} are scaled by this rate in order to non-dimensionalize.

The **carrying capacity** K of bacteria in a medium depends on the environment. Even within the sputum of patients with cystic fibrosis, the carrying capacity is difficult to estimate due to variability among patients. One study of patients with cystic fibrosis found that the densities of viable *P. aeruginosa* in sputum of 12 patients not undergoing treatment ranged from $5.3\text{e}3 \text{ CFU/mL}$ to $1.8\text{e}11 \text{ CFU/mL}$ [78].

The **infection rate** for *E. coli* and T4 phage in mucus (assuming mass action infection) is known to be approximately $47\text{e-}10 \text{ mL/min per CFU per PFU}$ [79, 80]. Infection in marine ecosystems (also assuming mass action infection) is similar at around $24\text{e-}10 \text{ mL/min per CFU per PFU}$ [77, 79]. Given our uncertainty in the bacterial carrying capacity, we elected to use an infection rate within the range given by Sinha et al. [26]; the authors fit their mass action infection model to time series population data that reached carrying capacity. The authors presented $K\eta \in [0.45, 100] \text{ hr}^{-1}$ and $r_S \in [0.5, 10] \text{ hr}^{-1}$. Non-dimensionalization leads to a range of η between 0.045 and 200, and our selected value of $\eta = 1$ is near the geometric mean of that range.

The **phage production delay rate** δ is estimated based on the eclipse and rise phase of PAXYB1 and PAK_P3 phage [46, 47]. The eclipse (latent) and rise phase is 130 minutes total for PAXYB1 [46] and 27 minutes total for PAK_P3 [47]. The smallest (non-dimensional) delay rate is then $1/130/5.1\text{e-}3 = 1.5$, and the largest is $1/27/5.1\text{e-}3 = 7.3$. We selected the approximate average of this range, 4, to be the delay rate.

The **phage degradation rate** μ_i is estimated based on the decay rates of phage in aquatic environments [43]. The decay rates ranged from 0.26 to 1.1 per hour. We non-dimensionalize by multiplying by 60 minutes per hour and the bacterial growth rate, $5.1\text{e-}3$ per minute. The non-dimensional range of decay rates is then 0.9 to 3.6. We selected a value of 1 arbitrarily from this range.

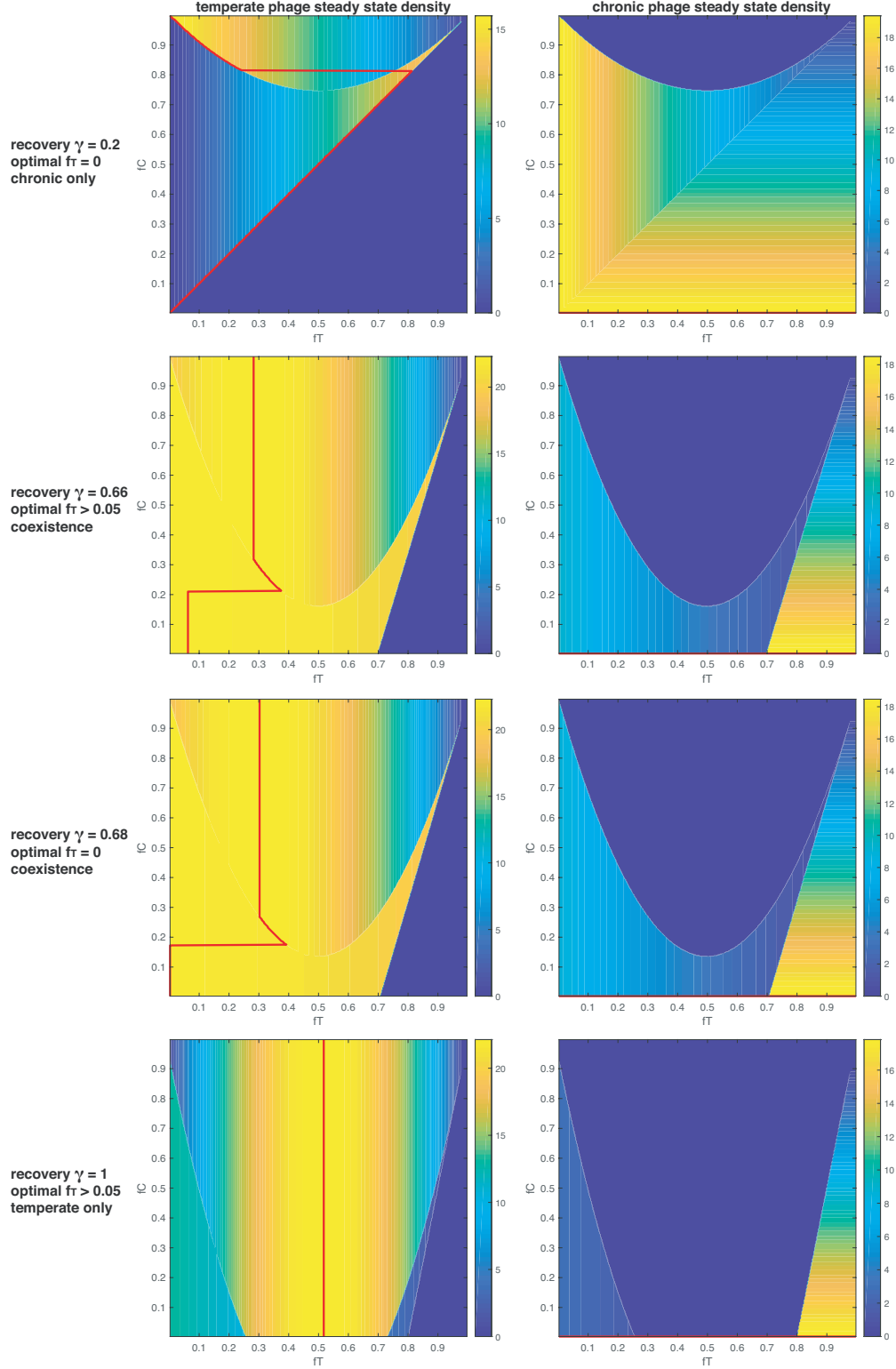


FIG. 5. Viral steady state density over the full range of possible lysogen frequencies ($f_i \in [0, 1]$) for temperate and chronic viruses. Color indicates the steady state viral density, and the red line is the maximum steady state density for each lysogen frequency of the competing virus. Left panel is temperate virus density ($V_T + L_T$) at steady state. Right panel is chronic virus density ($V_C + L_C$) at steady state. Top row is $\gamma = 0.2$, followed by $\gamma = 0.66$, $\gamma = 0.68$, and the bottom row is $\gamma = 1$.